Chemical Engineering Journal 362 (2019) 812–817

Contents lists available at ScienceDirect

Chemical Engineering Journal

journal homepage: www.elsevier.com/locate/cej

Short communication

Multi-graded foams upon time-dependent exposition to blowing agent

Marco Trofa, Ernesto Di Maio*, Pier Luca Maffettone

Dipartimento di Ingegneria Chimica, dei Materiali e della Produzione Industriale, University of Naples Federico II, P.le Tecchio 80, 80125 Naples, Italy

HIGHLIGHTS

- Time-varying b.c. of gas sorption stage induce multi-graded concentration profiles.
- At pressure release, said profiles result in multi-graded foam morphology profiles.
- Multi-graded foams are achieved via a simple upgrade of the gas foaming technology.

ARTICLE INFO

Keywords:
Foam
Layered
Graded
Carbon dioxide
Gas foaming

ABSTRACT

Layered and graded foams have proven superior to their uniform counterparts in terms of structural, and functional properties. This is also suggested by nature, abundant with porous material structures whose attributes are far beyond any artificial foam. To date, advanced foamed structures are generated via advanced though complex/time consuming technologies. Here we explore the possibility to generate layered and graded polymeric foams by using the simple gas foaming technology, with the sole introduction of time-varying boundary conditions of the gas sorption stage. We show that, by ingeniously designing the sorption step, it is possible to achieve non-trivial gas concentration profiles and, correspondingly, at pressure release, foams with density and/or morphology profiles. As a model system, we foamed polystyrene and polycaprolactone with CO_2 and N_2, and achieved three- as well as five-layered foams, gradually or sharply graded, yet in a single foaming step (pressure release) executed after different sorption protocols.

Thermoplastic foams are ubiquitous in daily life, as well as in the industry and technology, due to their *versatility,* low *cost* and *performances*. Not to mention the variety of foamable polymers, versatility derives from the possibility to tune foam *density* and *morphology* to the specific application. Reduced costs, with respect to unfoamed, dense polymers, arise essentially from the possibility to reduce material usage and parts weight. These advantages, of course, are obtained without sacrificing performances. Furthermore, foams are often the optimal material solution to boost performances on a constant weight basis. Nature, which has improved material usage during millions of years of evolution, is in fact crowded with porous materials, for the functional and the structural properties as well: wood, bones, shellfish shells, the Nature structural materials, all are porous materials. At a closer look, in fact, natural high-performance porous materials have a complex structure, non-uniform in the density and/or the morphology, e.g., to cope with the graded stress fields arising in the practical loading conditions or with the directional transport of nutrients [1].

Scientists are trying to mimic these structures, and several strategies are reported to achieve foams with graded densities and/or morphologies [2–9]. Some of the reported strategies, however, look a bit factitious, and difficult to scale-up. Graded microballoon positioning [10], multiple foamed layers gluing [11], localized bubble nucleation [6] and moulding under temperature gradients [4] are some examples, which, together with numerous theoretical studies [12–16], point to the improved structural and functional properties of the graded foams with respect to the uniform ones. Potentially easier to scale-up, the use of a "Non-Equilibrium gas concentration Profile", NEP, was introduced by Zhou et al. [17] and considers shortcutting the gas sorption step of the *gas foaming process* to attain non-uniform foams. In the gas foaming process, sorption of the blowing agent – typically a gas, for example CO_2 or N_2 – is a key step preceding foaming and is conducted at high, *constant*, pressure for a sufficient period of time (sorption time is close to, but larger than the characteristic diffusion time, τ_d, in this diffusion-controlled problem – $\tau_d = L^2/D$, where L is the sample thickness and D is the gas diffusivity in the polymer matrix). When pressure is quickly released, the solubilized gas nucleates the bubbles, whose *size* and *number density* depend on the gas concentration. If sorption time is less than τ_d, a NEP, whose 3D geometry depends on sample size, shape and

* Corresponding author.
E-mail address: edimaio@unina.it (E. Di Maio).

https://doi.org/10.1016/j.cej.2019.01.077
Received 10 October 2018; Received in revised form 6 January 2019; Accepted 12 January 2019
Available online 16 January 2019
1385-8947/

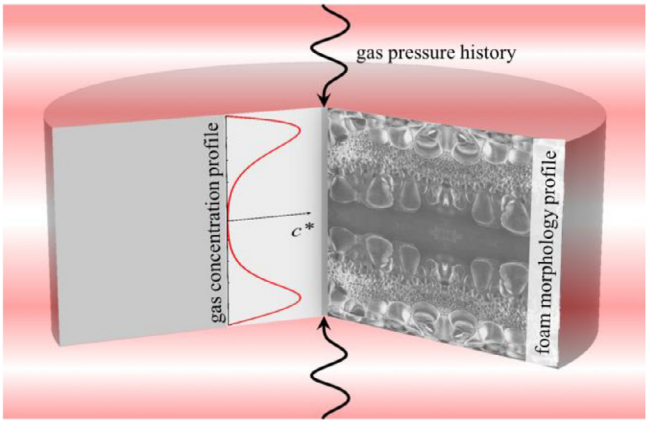

Fig. 1. Rationale of the proposed method. Applying a time-varying external gas pressure – gas pressure history – to a polymeric sample (cylindrical, in this scheme) results in a 3D gas concentration profile evolving, during the sorption stage, with a characteristic time τ_d O(100 min). If the characteristic time of the pressure change (e.g., a periodic wave with period T O(1 min)) is less than τ_d, it is possible to design the NEP to a certain extent. When the external pressure is rapidly O(0.01 s) quenched to atmospheric pressure, the super-saturated NEP induces bubble formation to an extent that depends locally on the instantaneous gas concentration.

the gas-accessible surfaces, will establish. The NEP will result, at the pressure release, in a corresponding bubble size and number density profile: a graded foam. Despite the ease of achievement of a graded structure, this method is, however, quite limited, as it does not allow anything different from a single-graded structure, less foamed, because of a minor gas concentration, in the inner of the sample and fully foamed in the proximity of the surfaces in contact with the gas pressure.

In this paper, we push forward the idea of using NEPs to achieve multiple graded (layered) foamed structures. In particular, the novel method relies on the application of time-varying boundary conditions in the mass transport of the blowing agent, thereby revealing a portfolio of possible NEPs. At the pressure release, the different NEPs will result in foams with different layering in terms of morphology and/or density, unconceivable with so-far utilized constant-pressure sorption (Fig. 1).

To design the sorption step to achieve the desired NEP, the above problem of diffusion in a slab of thickness L (see Fig. 2a), made impermeable on the lateral surface $\partial\Omega_W$ and accessible to the blowing agent through the surfaces $\partial\Omega_1$ and $\partial\Omega_2$, can be described by a one-dimensional Fickian model (reasonable in the sorption of low molecular weight penetrants in rubbery polymers [18]) with time varying boundary conditions:

$$\frac{\partial c}{\partial t} = D\frac{\partial^2 c}{\partial x^2}, \quad 0 < x < L$$

$$b.\,c. \quad \begin{matrix} c(0,\,t) = \phi_1(t) \\ c(L,\,t) = \phi_2(t) \end{matrix}$$

$$i.\,c. \quad c(x,\,0) = f(x) = c_0$$

where we have assumed constant L and gas diffusivity D, and a uniform initial gas concentration c_0. Although a more accurate model could include swelling and a concentration dependent diffusivity, we are here interested in a preliminary qualitative description. This problem has a general analytical solution [19] (see Supplementary material). If we consider, on both sides of the sample, a periodic boundary condition of period T, and we make the equations dimensionless by using T as the characteristic time and L as the characteristic length, the following dimensionless parameter arises $\Pi = DT/L^2$.

This number can be seen as the ratio between the characteristic time of the boundary condition T and the characteristic time of diffusion L^2/D, or the square of the ratio between the penetration depth (corresponding to one period) $\sqrt{(DT)}$ and the sample size L. The other parameter which has to be taken into account is the total process time $t_f^* = t_f/T$, i.e., the total number of periods. The time evolution of the dimensionless concentration profile c^* (normalized as respect to saturation) inside an initially empty sample, with a sinusoidal boundary condition $\phi^*(t^*) = 0.5(1 + \sin(2\pi t^* - \pi/2))$ on both sides, and for different values of the parameter Π is reported in Fig. 2b. Only half of the sample is considered for symmetry. When $\Pi \sim 1$ (top panel) the boundary condition varies so slowly that the concentration inside the sample has the time to reach equilibrium and the profile is almost uniform (quasi-steady-state). In this condition, there is no difference at increasing the number of periods considered. When reducing Π, e.g., by using a higher frequency boundary condition, the penetration depth decreases and concentration gradients arise (middle panel). The core of the sample is initially unaffected by the concentration variation at the boundary, however, as the number of periods increases (bottom panel), also the concentration inside the core starts to change, finally approaching the mean value of ϕ^*, i.e., $c^* = 0.5$. Similar trends can be calculated for a spherical sample. Hence, since we want to maximize gradients, which are progressively smoothed by diffusion, we will consider fast varying boundary conditions ($\Pi \ll 1$) and few oscillations ($t_f^* \sim 1$). Clearly, larger gradients are expected closer to the boundaries, where the variations are induced. In this regard, the most efficient pressure profile in creating gradients inside the sample is the square wave function. Reversed concentration profiles can also be obtained starting from a saturated sample.

Once the relevant variables and dimensionless number at play have been analysed and various possible NEPs drawn, we performed the foaming tests to verify the efficacy of the proposed method to achieve layered foams. Results will be reported, for the different cases, as in Fig. 3a, illustrating the tight correspondence between the NEP (as a consequence of a specific saturation pressure history) and the morphology of the foam. The morphology is reported through a Scanning Electron Microscopy (SEM) image and the qualitative analysis of the SEM image in terms of the bubble number density, N_b, and the average bubble size, Φ, profiles. The equipment utilized in this study is a custom-made instrumented pressure vessel capable of an accurate control of the processing variables (foaming temperature, saturation pressure and pressure drop rate). In particular, the saturation pressure program, key in this study, is achieved by computer control of a standard syringe pump (Fig. 3b). Samples used in this study are dual: slabs and beads, with cylindrical and spherical symmetry, respectively (Fig. 3c), made out of a foaming-grade polystyrene, PS. CO_2, N_2, and R-134a were utilized as the blowing agents. For the sake of clarity and proper comparison with the state of the art, we first achieved a standard foam, that is a uniform foam (Fig. 3a). This was obtained by pressure quenching a high-pressure polymer/gas solution with a spatially constant gas concentration attained after a long sorption step (sorption time $> \tau_d$) at constant pressure.

Also known in the state of the art, a simple graded foam was obtained by shortcutting the sorption stage, at constant pressure on an initially empty polymer. The resulting gas concentration profile is described by the *erf* function. At the pressure release, a N_b profile, faithfully following the NEP, results (the bubble nucleation rate monotonically increases with the gas concentration). Φ has the opposite trend, as the larger the N_b, the less gas is available to inflate each bubble. In particular, numerous tiny bubbles are observed close to the sample surface, gradually changing, towards the inner of the sample, to few large bubbles and, beyond, to a bulk unfoamed structure (Fig. 4a). As a development of known prior art, we now apply time-varying gas pressures to achieve foams with a desired, advanced, morphology (Fig. 4b-e). For example, if a more uniform external layer in the outer shell is desired with respect to the previous case, after a first sorption step at constant pressure (p_1 for a period $\ll \tau_d$), pressure has to be step-changed to a minor pressure p_2 for a period $\approx (p_2/p_1)(L^2/D)$ in order to partially empty the external layers. If p_2 is sufficiently close to p_1, then

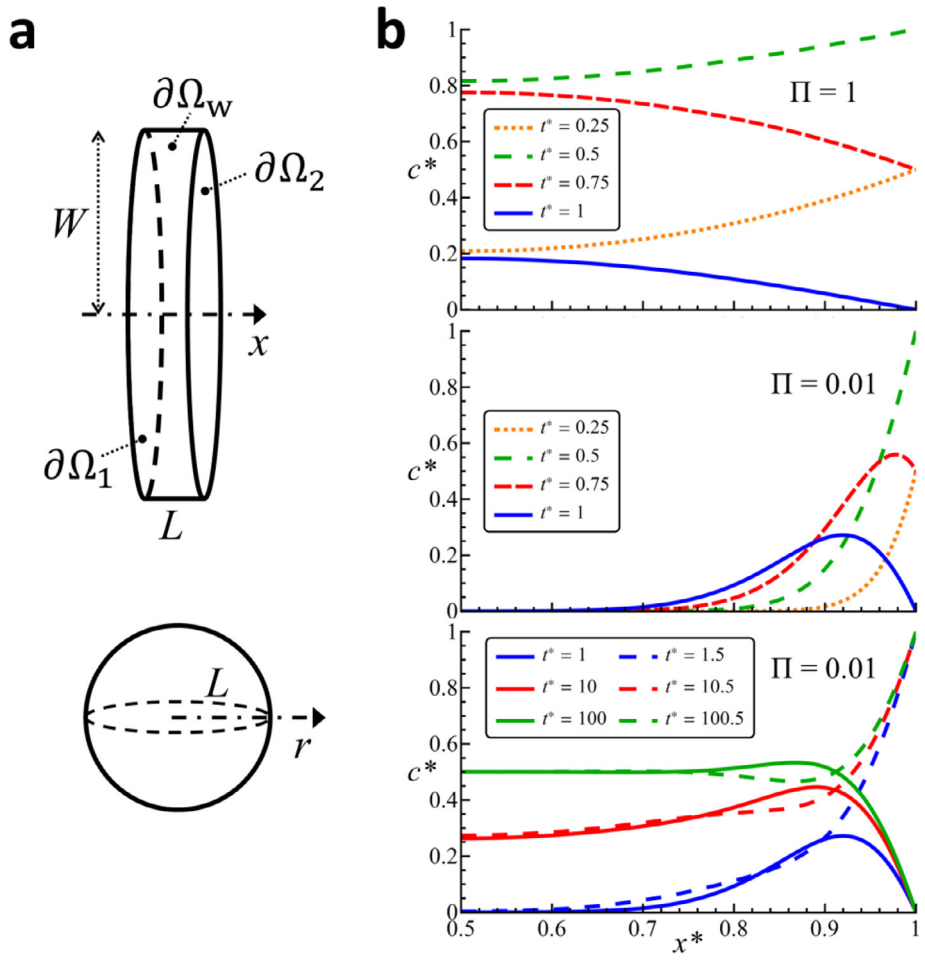

Fig. 2. Modelling of the sorption with time-dependent boundary conditions. **a**, Adopted geometries. **b**, Time evolution of the NEP for different Π. Only half of the sample is considered for symmetry. The concentration is normalized as respect to saturation.

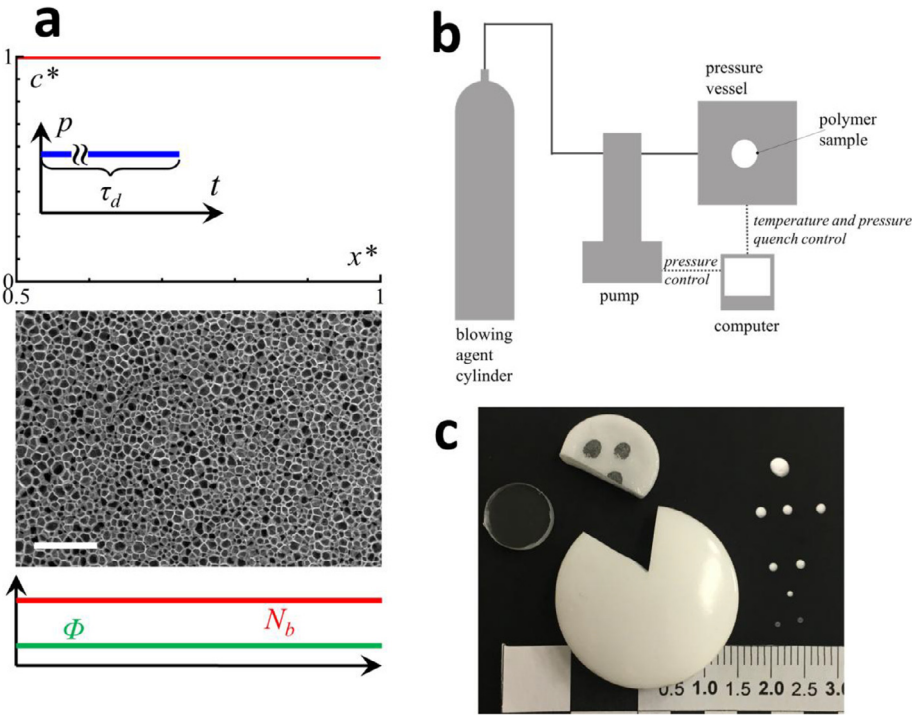

Fig. 3. Gas foaming of thermoplastics. **a**, Top image: in "state-of-the-art" gas foaming of thermoplastics, the external gas pressure p is constant over time (inset) and, after a period longer than τ_d, a constant spatial c^* profile is achieved. Middle image: at pressure release, a uniform foam is achieved because of the constant concentration, as observed by SEM (scale bar is 500 μm); Bottom: N_b and Φ spatial profiles, to qualitatively describe the foam morphology. **b**, Schematic of the equipment adopted in the present study (Supplementary Methods gives details). **c**, Samples before and after foaming. On the left, the transparent polystyrene slab before foaming and two white foamed slabs (pieces were removed for analysis); on the bottom right, the small, transparent polystyrene spheres before foaming and some foamed spheres, top right.

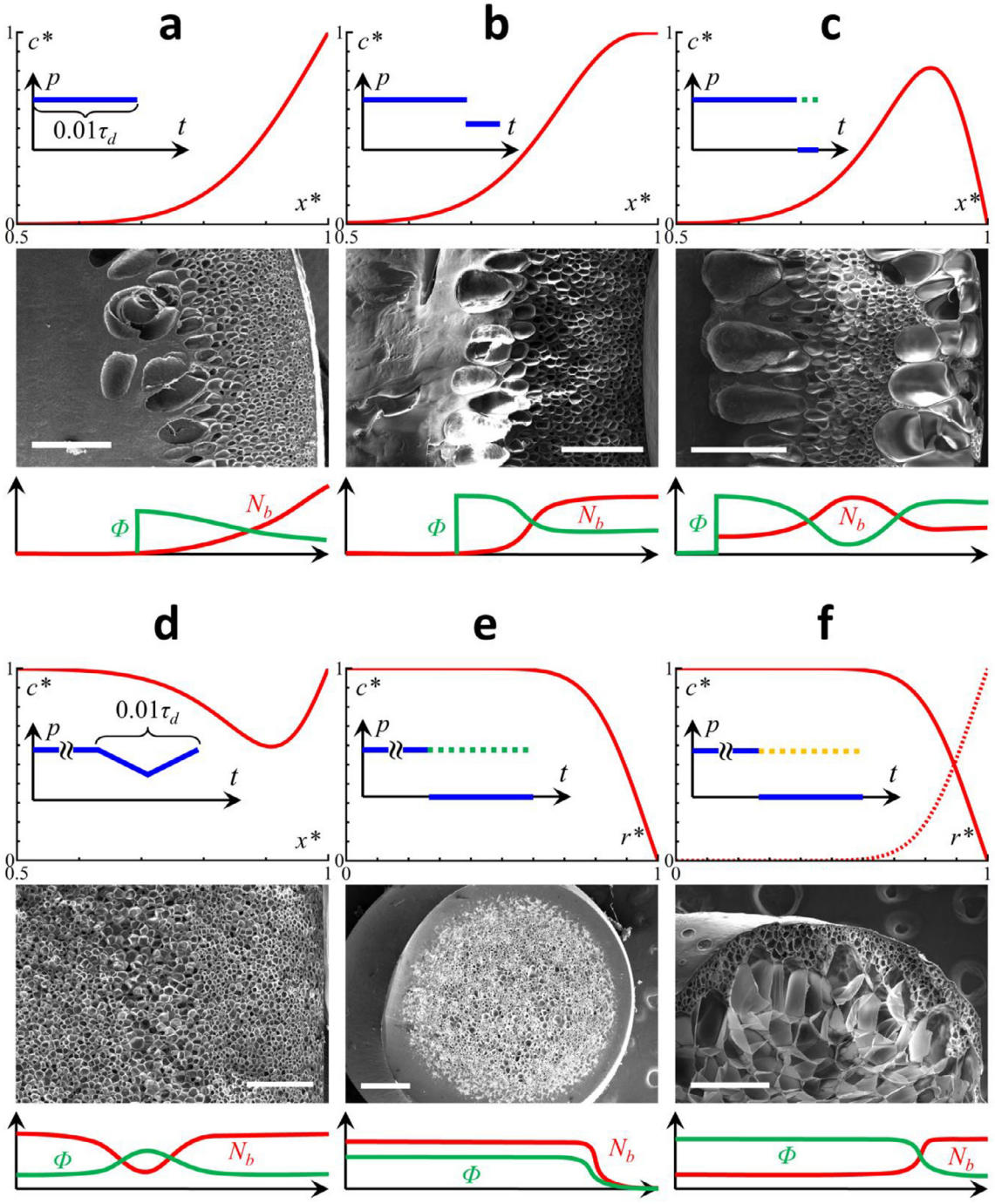

Fig. 4. Graded foams as a result of different NEP. top: normalized concentration profile (c^* vs. x^*) after a specific sorption pressure history (p vs. t in the inset); middle: corresponding SEM micrograph (scale bar is 500 μm); bottom: N_b and Φ qualitative profiles of the morphologies shown in the SEM image. **a**, constant CO_2 pressure sorption shortcutting as reported by Zhou et al. [17] **b**, to have a more uniform morphology in the outer foamed shell with respect to **a**, CO_2 pressure was halved before final pressure release. **c**, the outer shell can be also further emptied, by substituting, at constant pressure, the CO_2 with a much slower diffusing gas, R-134a, before final pressure release. **d**, after saturating the whole sample with CO_2 at constant pressure for a period longer than τ_d, applying a triangular pressure program results in partially emptying the outer shell of the sample in the decreasing pressure ramp and filling again the outmost shell in the increasing pressure ramp. **e**, like **d**, but by totally emptying the outer shell by substituting, at constant pressure, the CO_2 with R-134a, before final pressure release. **f**, like **e**, but with N_2 in the place of R-134a, as a substitute for CO_2, before the final pressure release. Samples **a** – **d** are slabs, **e** and **f** are spheres. In the insets, blue line is CO_2, orange is N_2 and green is R-134a. (For interpretation of the references to colour in this figure legend, the reader is referred to the web version of this article.)

no precautions are needed to avoid premature foaming during the second sorption step and the excess CO_2 just diffuses out of the sample, as the super-saturation is not sufficient to nucleate the new phase. If a less foamed-to unfoamed external layer is desired, then a gas switch is required, maintaining a constant p_1. In particular, we utilized a slow-diffusing gas, because of a higher molecular weight – namely R-134a – to substitute CO_2 at constant pressure. This results in a CO_2 emptying of the outer layer, without premature foaming, which is eventually achieved at pressure quench after the required emptying period elapsed (Fig. 4c). The graded foams examples depicted so far were achieved on samples which were initially empty, i.e., at $c_0 = 0$. The following examples regard samples initially at a (high) gas concentration (they were

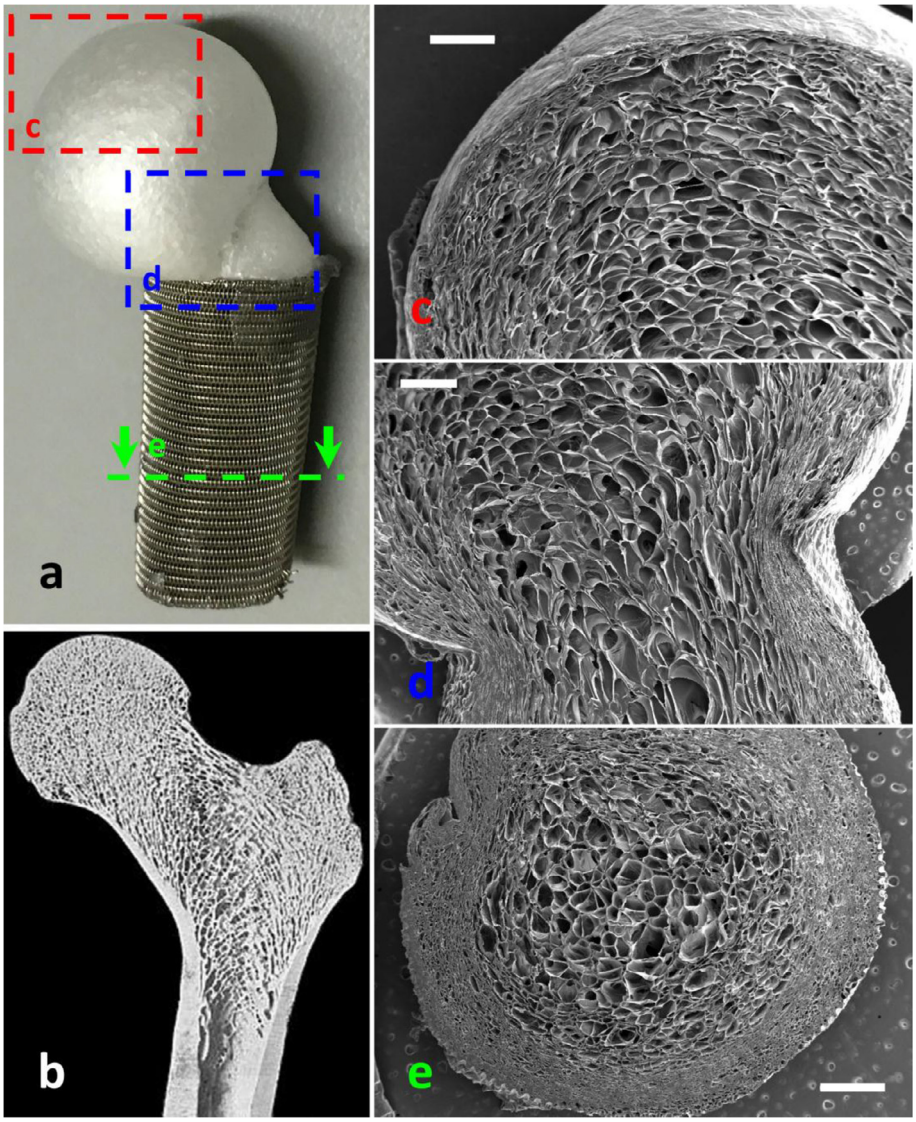

Fig. 5. Graded foams in the biomimicry of a femur. **a**, femur-like foam showing the porous rigid metallic net containing the sample. The dashed lines denote the sections reported in **c** (red), **d** (blue), and **e** (green). **b**, picture of a femur section, showing the complex porosity architecture of the natural bone. **c**, **d**, and **e**, SEM images showing two longitudinal and a transversal cross section of the sample (scale bar is 1 mm). (For interpretation of the references to colour in this figure legend, the reader is referred to the web version of this article.)

saturated at a constant, high pressure for a period $> \tau_d$). In particular, it is possible to modify the uniform morphology of Fig. 3a, by inducing a concentration reduction (increase) with a pressure reduction (increase). The depth of the layer where this morphology change is attained can be to a certain extent designed, by restoring the initial pressure and by adjusting timing and shape of the pressure history profile. If a triangular pressure profile is applied at the end of the sorption stage, a 5-layers morphology is achieved (Fig. 4d); if the external layer has to be stiff or impermeable, it is possible to render it bulk by substituting CO_2 with R-134a at constant pressure (Fig. 4e); finally if the external layer has to have a different morphology than the inner of the sample, then it is sufficient to substitute the CO_2 with a different, yet effective foaming agent, N_2, capable of giving finer morphologies (Fig. 4f).

At this point it is clear that many layered foamed structures are possible, keeping in mind that imagination is upper bounded by the physics of mass transport, as to have concentration gradients one has to hamper diffusion. Since we observed that the human bone has an extremely advanced porous structure, graded in both density and morphology, and with cells oriented in the loading directions, we were tempted to use this method to achieve a femur-like foam, of potential interest to the tissue engineering field (Fig. 5). We utilized, in this case, polycaprolactone, PCL, a biocompatible polyester extensively utilized in tissue engineering. For comparison we report a section of a real femur (Fig. 5b) and three sections of the femur-like sample (Fig. 5c-e). The graded density and morphology as such as the orientation were obtained by the use of a procedure similar to the case of Fig. 4f and with an open mould to herniate the head of the femur part.

It is important to note that, in order to achieve the desired Π when the size of the sample L increases, for using this method in real life applications, it is possible to adjust D, which exponentially varies with the temperature. Here, a possible limit of the technique can be foreseen based on the extent of the foaming processing window available with polymers. For a possible, further development, a-symmetries could also be investigated, e.g., by covering one side of the sample with a polymeric film of a different nature (e.g., a barrier film towards the blowing agent) or by using two different materials in contact with each other, or even by imposing, with some larger experimental hurdle, different pressure profiles or different gases on the sides of the sample. These novel materials can be exploited, for instance, to produce new safety

helmets, damping soles, and automotive bumper beams [20] with improved energy absorption performance and reduced weight. As a final remark, we believe that the idea of using time varying boundary conditions can be applied to any process involving mass as well as energy transport (e.g., drying and quenching) to develop new layered, advanced materials.

Data availability

The raw data required to reproduce these findings are available to download from https://data.mendeley.com/datasets/pywh2vyzvg/2.

Acknowledgements

Authors thank C. Boizet and F. Guarracino for cooperation in performing the experiments. The financial support of Materias S.r.l. is gratefully acknowledged.

Author contributions

E.D.M. conceived the work and performed the experiments, E.D.M. and M.T. analysed data, M.T. and P.L.M. developed the analytical model, and all the authors wrote the paper and commented on the article.

Competing interests

The authors declare that they have no competing interests.

Appendix A. Supplementary data

Supplementary data to this article can be found online at https://doi.org/10.1016/j.cej.2019.01.077.

References

[1] M.A. Meyers, J. McKittrick, P.-J. Chen, Structural biological materials: critical mechanics-materials connections, Science 339 (2013) 773–779.
[2] U.G.K. Wegst, H. Bai, E. Saiz, A.P. Tomsia, R.O. Ritchie, Bioinspired structural materials, Nat. Mater. 14 (2015) 23–36.
[3] D. Jones, Daedalus floating on nothing, Nature 389 (1997) 793.
[4] H. Bai, et al., Bioinspired large-scale aligned porous materials assembled with dual temperature gradients, Sci. Adv. 11 (2015) e1500849.
[5] H. Niknam, A.H. Akbarzadeh, D. Rodrigue, D. Therriault, Architected multi-directional functionally graded cellular plates, Mater. Des. 148 (2018) 188–202.
[6] J. Yu, et al., Preparation of polymer foams with a gradient of cell size: further exploring the nucleation effect of porous inorganic materials in polymer foaming, Mater. Today Commun. 9 (2016) 1–6.
[7] S.G. Mosanenzadeh, H.E. Naguib, C.B. Park, N. Atalla, Design and development of novel bio-based functionally graded foams for enhanced acoustic capabilities, J. Mater. Sci. 50 (2015) 1248–1256.
[8] N. Santamaria, et al., A randomised controlled trial of the effectiveness of soft silicone multi-layered foam dressings in the prevention of sacral and heel pressure ulcers in trauma and critically ill patients: the border trial, Int. Wound J. 12 (2015) 302–308.
[9] S.M. Giannitelli, et al., Graded porous polyurethane foam: a potential scaffold for oro-maxillary bone regeneration, Mater. Sci. Eng. C 51 (2015) 329–335.
[10] N. Gupta, W. Ricci, Comparison of compressive properties of layered syntactic foams having gradient in microballoon volume fraction and wall thickness, Mater. Sci. Eng. A Struct. Mater. 427 (2006) 331–342.
[11] E. Wang, N. Gardner, A. Shukla, The blast resistance of sandwich composites with stepwise graded cores, Int. J. Solids Struct. 46 (2009) 3492–3502.
[12] L. Cui, S. Kiernan, M.D. Gilchrist, Designing the energy absorption capacity of functionally graded foam materials, Mater. Sci. Eng. A 507 (2009) 215–225.
[13] G. Sun, G. Li, S. Hou, S. Zhou, W. Li, Q. Li, Crashworthiness design for functionally graded foam-filled thin-walled structures, Mater. Sci. Eng. A 527 (2010) 1911–1919.
[14] M.A. Forero Rueda, L. Cui, M.D. Gilchrist, Optimisation of energy absorbing liner for equestrian helmets. Part I: Layered foam liner, Mater. Des. 30 (2009) 3405–3413.
[15] J.F. Allard, C. Depollier, P. Rebillard, Inhomogeneous Biot waves in layered media, J. Appl. Phys. 66 (1989) 2278.
[16] H. Liu, Z. Zhang, H. Liu, J. Yang, H. Lin, Theoretical investigation on impact resistance and energy absorption of foams with nonlinearly varying density, Compos. B Eng. 116 (2017) 76–88.
[17] C. Zhou, P. Wang, W. Li, Fabrication of functionally graded porous polymer via supercritical CO2 foaming, Compos. B Eng. 42 (2011) 318–325.
[18] S. Matteucci, Y. Yampolskii, B.D. Freeman, I. Pinnau, Materials Science of Membranes for Gas and Vapor Separation, John Wiley & Sons, Chichester, 2006.
[19] H.S. Carslaw, J.C. Jaeger, Conduction of Heat in Solids, Oxford Science Publications, Oxford, 1959.
[20] Z. Xiao, J. Fang, G. Sun, Q. Li, Crashworthiness design for functionally graded foam-filled bumper beam, Adv. Eng. Software 85 (2015) 81–95.